

A Colorful Wake for Gerhard Soff

Berndt Müller and Jörg Ruppert

Department of Physics, Duke University, Durham, NC 27708, USA

Abstract. We calculate the wake induced in a hot QCD plasma by a fast parton in the framework of linear response theory. We discuss two scenarios: (i) a weakly coupled quark-gluon plasma described by hard-thermal loop perturbation theory and (ii) a strongly coupled quark-gluon plasma which resembles a quantum liquid. We show that a Mach cone can appear in the second scenario, but not in the first one.

1. Introduction

The Oxford English Dictionary records three different meanings of the noun *wake*:

- a trail of disturbed water or air left by the passage of a ship or aircraft;
- a watch or vigil held beside the body of someone who has died;
- (especially in Ireland) a party held after a funeral.

Since the Greek word *συμπόσιον* describes a gathering of friends to eat, drink, and converse, the *Symposium* in memory of our deceased friend and colleague Gerhard Soff certainly fits the third definition. My lecture will be mainly concerned with the first definition, in a slightly generalized sense. To define the appropriate context, we first need to review some of the salient results from the experiments conducted at the Relativistic Heavy Ion Collider (RHIC).

The quenching of QCD jets in relativistic heavy ion collisions due to the energy loss suffered by hard partons as they traverse dense matter was proposed more than two decades ago as an important indicator for the creation of a quark-gluon plasma [1, 2, 3]. Over the past five years, this phenomenon has been extensively studied experimentally at RHIC. One looks for hadrons with a high transverse momentum p_T , which are produced when an energetic, hard scattered parton fragments into hadrons far outside the remnants of the nuclear collision. Since both, the scattering probability and the fragmentation probability, are known or calculable in QCD, the sole unknown is the amount of energy lost by the parton before it fragments into hadrons. This makes it possible to deduce the energy loss from the measured hadron yield.

The RHIC data clearly demonstrate a strong suppression of the emission of high- p_T hadrons in Au + Au collisions. The suppression is found to grow in severity with increasing

centrality. The suppression factor R_{AA} , defined as the ratio of the hadron yield in Au + Au collisions compared to the yield in $p + p$ collisions scaled by the appropriate number of binary nucleon-nucleon interactions in the nuclear collision, reaches about 1/5 in the most central events [4]. Most of the observed hadrons originate near the surface of the interaction region oriented toward the detector. Hadrons from the companion jet emitted in the opposite direction, which has a much longer path through the medium, are even more strongly suppressed [5].

The main emphasis in theoretical studies of jet quenching has been on the description of the energy loss which the leading parton suffers due to the emission of a secondary partonic shower when traversing the medium. Reviews of the theory of medium induced energy loss and its associated phenomenology are found in [7, 8, 9, 10]. The main result is that the energy loss of a hard parton in dense QCD matter is dominated by radiative processes involving gluon emission after elastic collisions of the parton with color charges (mostly gluons) contained in the medium. Coherence effects lead to a quadratic dependence of the total energy loss on the traversed path length L . The stopping power of the medium is encoded in the quantity

$$\hat{q} = \rho \int q^2 \frac{d\sigma}{dq^2} dq^2, \quad (1)$$

where ρ denotes the gluon density of the medium and $d\sigma/dq^2$ is the differential cross section for elastic scattering.

An interesting question is: What happens to the radiated energy? Or more generally: How does the medium respond to the penetration by the hard parton? The RHIC experiments are just beginning to address this intriguing question. First indications of a medium response have been seen in three sets of data:

1. Although energetic hadrons in the direction opposite to a high- p_T trigger hadron are almost completely suppressed in central collisions [5], one finds an increased yield of soft, low- p_T hadrons [11, 12].
2. The angular distribution of the soft hadrons emitted in the direction opposite to an energetic hadron does not seem to peak at 180° but at a smaller angle [13, 14].
3. Correlated two-hadron emission in the same direction in the momentum range $0.15 \text{ GeV}/c < p_T < 2 \text{ GeV}/c$ is enhanced [15].

Since the quark-gluon plasma is a plasma, after all, it is natural to begin a theoretical investigation of the medium response by applying the tools which have been successfully used to describe the response of a metallic electron plasma to the penetration by a fast ion. Such a charged projectile induces a wake of charge and current density in the target, accompanied by induced electric and magnetic fields. The wake, which has the shape of a Mach cone, reflects significant aspects of the response of the medium.

After a brief review of the evidence for this phenomenon in condensed matter physics, we apply the same methods of linear response theory to the system of a relativistic color charge traveling through a QCD plasma. We calculate the plasma response to an external point source traveling at a velocity close to the speed of light. In this framework, quantum

effects are included implicitly via the dielectric functions, ε_L and ε_T . For simplicity, we shall assume that the medium is homogeneous and isotropic, and we disregard finite size effects. We then consider two models for the color response of the QCD plasma: (i) the response predicted by QCD perturbation theory, and (ii) a response of the kind expected for a strongly coupled, “liquid” plasma. We present the results of our calculations of the wake structure behind a fast color charge for both scenarios and discuss the general conditions which must be met for the wake to have a Mach cone-like structure [16, 17].

2. Plasma linear response theory

The linear response of the plasma to an external electromagnetic field has been extensively studied in plasma physics (see e. g. [18]). In this formalism, a dielectric medium is characterized by the components of the dielectric tensor $\varepsilon_{ij}(\omega, k)$. For an isotropic, homogenous medium the dielectric tensor can be decomposed into its longitudinal and transverse components characterized by the dielectric functions $\varepsilon_L(\omega, k)$ and $\varepsilon_T(\omega, k)$:

$$\varepsilon_{ij} = \varepsilon_L \mathcal{P}_{L,ij} + \varepsilon_T \mathcal{P}_{T,ij}. \quad (2)$$

Here $\mathcal{P}_{L,ij} = k_i k_j / k^2$ and $\mathcal{P}_T = 1 - \mathcal{P}_L$ are the longitudinal and transverse orthonormal projectors with respect to the momentum vector \vec{k} . One can relate the dielectric functions ε_L and ε_T to the self-energies Π_L and Π_T of the in-medium photon via [19]:

$$\varepsilon_L(\omega, k) = 1 - \frac{\Pi_L(\omega, k)}{\omega^2 - k^2}, \quad \varepsilon_T(\omega, k) = 1 - \frac{\Pi_T(\omega, k)}{\omega^2}. \quad (3)$$

Using Maxwell’s equations and the continuity equation in momentum space, the total electric field \vec{E}_{tot} in the plasma is related to the external current \vec{j}_{ext} via:

$$\left[\varepsilon_L \mathcal{P}_L + \left(\varepsilon_T - \frac{k^2}{\omega^2} \right) \mathcal{P}_T \right] \vec{E}_{\text{tot}}(\omega, k) = \frac{4\pi}{i\omega} \vec{j}_{\text{ext}}(\omega, k). \quad (4)$$

Equation (4) has propagating solutions when the determinant constructed from the elements of the tensor vanishes:

$$\det \left[\varepsilon_L \mathcal{P}_L + \left(\varepsilon_T - \frac{k^2}{\omega^2} \right) \mathcal{P}_T \right] = 0. \quad (5)$$

This equation governs the dispersion relation for the waves in the medium. It can be diagonalized into purely longitudinal and transverse parts, yielding dispersion relations for the longitudinal and transverse dielectric functions [18]:

$$\varepsilon_L(\omega, k) = 0, \quad \varepsilon_T(\omega, k) = (k/\omega)^2. \quad (6)$$

These equations determine the longitudinal and transverse plasma modes. The longitudinal equation is the dispersion relation for density fluctuations in the plasma, namely space-charge fields which can propagate through the plasma without far away from an external perturbation.

The charge density induced in the wake by the external charge distribution is:

$$\rho_{\text{ind}} = \left(\frac{1}{\epsilon_L} - 1 \right) \rho_{\text{ext}}. \quad (7)$$

In the transverse gauge, the induced charge density is related to the induced Coulomb potential via the Poisson equation: $k^2 \Phi_{\text{ind}} = 4\pi \rho_{\text{ind}}$. Since one can relate the total electric field to the induced charge in linear response theory by

$$\vec{j}_{\text{ind}} = \frac{i\omega}{4\pi} (1 - \epsilon) \vec{E}_{\text{tot}}, \quad (8)$$

a direct relation between the external and the induced current can be derived using (4):

$$\vec{j}_{\text{ind}} = \left[\left(\frac{1}{\epsilon_L} - 1 \right) \mathcal{P}_L + \frac{\omega^2 (1 - \epsilon_T)}{\omega^2 \epsilon_T - k^2} \mathcal{P}_T \right] \vec{j}_{\text{ext}}. \quad (9)$$

The induced charge and the induced current obey the continuity equation:

$$i\vec{k} \cdot \vec{j}_{\text{ind}} - i\omega \rho_{\text{ind}} = 0. \quad (10)$$

Finally, we need to specify the form of the external current. For a fully stripped ion (or a single energetic parton) it is appropriate to assume the current and charge density of a point-like charge moving along a straight line trajectory with constant velocity \vec{v} , whose Fourier transform is given by [20]:

$$\begin{aligned} \vec{j}_{\text{ext}} &= 2\pi q \vec{v} \delta(\omega - \vec{v} \cdot \vec{k}), \\ \vec{\rho}_{\text{ext}} &= 2\pi q \delta(\omega - \vec{v} \cdot \vec{k}). \end{aligned} \quad (11)$$

All equations given above, from (2) to (11), immediately generalize to QCD by the simple addition of a color index $a = 1, \dots, 8$ to the charge, the current, and the field strength, which are all in the adjoint representation of color SU(3) :

$$q \rightarrow q^a, \quad (\rho, \vec{j}) \rightarrow (\rho^a, \vec{j}^a), \quad \vec{E} \rightarrow \vec{E}^a. \quad (12)$$

Since we are limiting the treatment of the medium response to effects that are linear in the perturbation, all nonlinear terms arising from the nonabelian nature of the color field are discarded. The strength of the color charge of the projectile is defined by $q^a q^a = C_2 \alpha_s$ with the strong coupling constant $\alpha_s = g^2/4\pi$ and the quadratic Casimir invariant C_2 ($C_F = 4/3$ for a quark or antiquark and $C_A = 3$ for a gluon). In this linearized treatment one disregards changes of the color charge while the particle is propagating through the medium. The non-abelian character of the QCD plasma only enters indirectly via the chromo-dielectric functions $\epsilon_{L/T}(\omega, k)$, which are scalars in color space [21, 22, 23]. Due to the self-interacting nature of the gluon in SU(3), gluons contribute to the polarization of the medium; in fact, they make the largest contribution.

The non-radiative part of the energy loss of the incident (color) charge is given by the back reaction of the induced (chromo-)electric field onto the incident particle. The energy loss per unit length is given by [18]:

$$\frac{dE}{dx} = q \frac{\vec{v}}{v} \text{Re} \vec{E}_{\text{ind}}(\vec{x} = \vec{v}t, t), \quad (13)$$

where the induced electric field \vec{E}_{ind} is the total electric field minus the vacuum contribution. Using the inverse of (4), the induced field is given by:

$$\vec{E}_{\text{ind}} = \left[\left(\frac{1}{\epsilon_L} - 1 \right) \mathcal{P}_L + \left(\frac{\omega^2}{\omega^2 \epsilon_T - k^2} - \frac{\omega^2}{\omega^2 - k^2} \right) \mathcal{P}_T \right] \frac{4\pi}{i\omega} \vec{j}_{\text{ext}}. \quad (14)$$

From (13) and (14) the non-radiative energy loss per unit length is given by [23]:

$$\frac{dE}{dx} = -\frac{C\alpha_s}{2\pi^2 v} \int d^3k \frac{\omega_k}{k^2} [\text{Im} \epsilon_L^{-1} + (v^2 k^2 - \omega_k^2) \text{Im} (\omega_k^2 \epsilon_T^{-1} - k^2)^{-1}], \quad (15)$$

where $\omega_k = \vec{v} \cdot \vec{k}$.

3. Quick flashback: Electron wakes in metal foils

The formation of electromagnetic wakes induced by a fast ion in the electron plasma of a thin metal foil was investigated starting around 1980 by Groeneveld and collaborators at Frankfurt [24, 25]. Their study was motivated, in part, by calculations [26, 27] done by a graduate student, Wolfgang Schäfer,¹ who had solved the equations of the previous section for a dielectric function of the Bloch type [28]

$$\epsilon_L = 1 + \frac{\omega_p^2}{u^2 k^2 - \omega^2} \quad (k \leq k_c), \quad (16)$$

where ω_p is the plasma frequency and u denotes the sound velocity in the plasma. The calculations showed that the wake in the electron plasma has the form of a Mach cone, similar to the Mach shock phenomena predicted for relativistic nucleus-nucleus collisions [29, 30]. In our publications, we not only showed the detailed shape of the spatial distribution of induced plasma charge and current (see Fig. 1), but we also predicted the angular distribution of the electrons which would be emitted when the current wave hits the surface of the metal foil (see Fig 1). The peak of this distribution roughly coincides with the ‘‘Mach angle’’, given by

$$\varphi_M = \arccos(u/v). \quad (17)$$

The first published data confirmed the presence of directed electron emission, and the dependence of the peak angle on the beam energy qualitatively agreed with our predictions [24]. However, it turned out that the results were not well reproducible unless the surface of

¹Before doing this work for his doctoral thesis, Wolfgang had worked under Gerhard Soff’s supervision calculating the influence of the vacuum polarization potential on the motion of two colliding heavy nuclei.

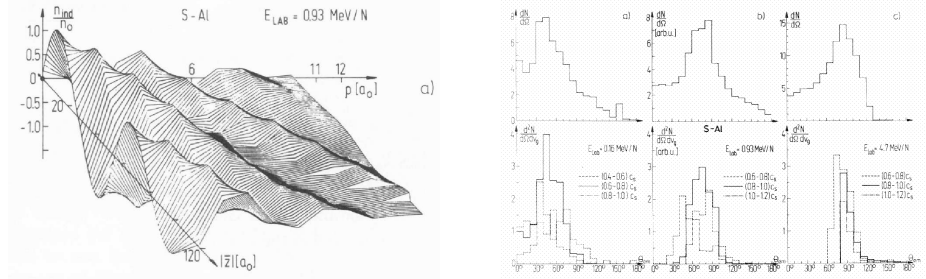


Fig. 1. Left: Spatial distribution of the induced charge density behind an ion traveling through a metal. The plot represents a radial cut through the Mach cone. Right: Predicted angular distribution of the electrons contained in the wake current.

the foil was extremely clean. Groeneveld's team therefore later repeated the measurement with foils whose surface had been sputter-cleaned. The new data (see Fig. 2) showed much more pronounced and reproducible peaks [25]. Their positions as a function of beam energy and Fermi energy of the target nicely followed the Mach relation (17) in agreement with the predictions [27].

The experimentalists continued to study many aspects of this phenomenon in great detail, including the energy spectra and angular distributions of the ejected electrons, the refraction of the Mach wave at the planar surface of the foil, and the response of high T_c superconductors [31]. In recent years, the collective plasma waves excited by fast ions in soft biological tissue have been considered as a mechanism that contributes to the damage to living cells by fast C^{6+} ions [32], which is an important factor in cancer therapy with heavy ion beams [33].

4. Color wake in the high temperature approximation

We now return to the problem of interest to us: the medium response to an energetic parton. We shall discuss two qualitatively different scenarios. We first assume that the plasma is in the weakly coupled high temperature regime, where the gluon self-energy can be described by the leading order of the high temperature expansion, $T \gg \omega, k$, commonly called the hard-thermal loop (HTL) approximation [34, 35]. This regime can be expected to be realized far above the deconfinement temperature T_c . The dielectric functions read [22, 21]:

$$\varepsilon_L = 1 + \frac{2m_g^2}{k^2} \left[1 - \frac{1}{2}x \left(\ln \left| \frac{x+1}{x-1} \right| - i\pi\Theta(1-x^2) \right) \right], \quad (18)$$

$$\varepsilon_T = 1 - \frac{m_g^2}{\omega^2} \left[x^2 + \frac{x(1-x^2)}{2} \left(\ln \left| \frac{x+1}{x-1} \right| - i\pi\Theta(1-x^2) \right) \right], \quad (19)$$

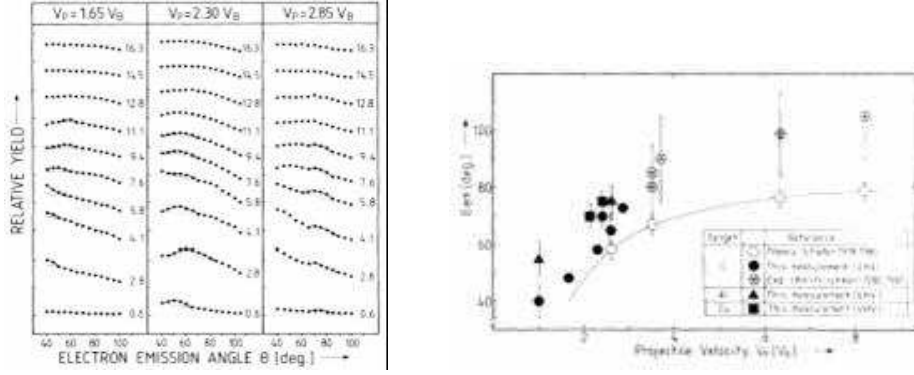


Fig. 2. Left: Angular distribution of electrons emitted after bombardment of thin metal foils by fully stripped ions. Right: Dependence of the peak position in the angular distribution for various target materials (C, Al, Cu) and different beam energies, in comparison with the predicted Mach angle for a carbon target (from [25]).

where $x = \omega/k$. We first discuss the induced charge and current densities ρ_{ind} and \vec{j}_{ind} . The Fourier transform of (7) in cylindrical coordinates is given by:

$$\rho_{\text{ind}}^a(\rho, z, t) = \frac{m_g^3 q^a}{(2\pi)^2 v} \int_0^\infty d\kappa' \kappa' J_0(\kappa \rho) \times \int_{-\infty}^\infty d\omega' \exp\left[i\omega\left(\frac{z}{v} - t\right)\right] \left(\frac{1}{\epsilon_L} - 1\right), \quad (20)$$

where $k = \sqrt{\kappa^2 + \omega^2/v^2}$ and $\omega = m_g \omega'$, $\kappa = m_g \kappa'$. This shows that the induced charge density ρ_{ind}^a is proportional to m_g^3 . The cylindrical symmetry around the jet axis restricts the form of the current density vector \vec{j}_{ind}^a . It only has non-vanishing components parallel to the beam axis:

$$j_{v,\text{ind}}^a(\rho, z, t) = \frac{m_g^3 q^a}{(2\pi)^2 v^2} \int_0^\infty d\kappa' \kappa' J_0(\kappa \rho) \int_{-\infty}^\infty d\omega' \exp\left[i\omega\left(\frac{z}{v} - t\right)\right] \left[\left(\frac{1}{\epsilon_L} - 1\right) \frac{\omega^2}{k^2} + \frac{1 - \epsilon_T}{\epsilon_T - \frac{k^2}{\omega^2}} \left(v^2 - \frac{\omega^2}{k^2}\right) \right], \quad (21)$$

and radially perpendicular to the beam axis:

$$j_{\rho,\text{ind}}^a(\rho, z, t) = \frac{i m_g^3 q^a}{(2\pi)^2 v} \int_0^\infty d\kappa' \kappa' J_1(\kappa \rho) \int_{-\infty}^\infty d\omega' \exp\left[i\omega\left(\frac{z}{v} - t\right)\right] \frac{\omega \kappa}{k^2} \left[\left(\frac{1}{\epsilon_L} - 1\right) - \left(\frac{1 - \epsilon_T}{\epsilon_T - \frac{k^2}{\omega^2}}\right) \right]. \quad (22)$$

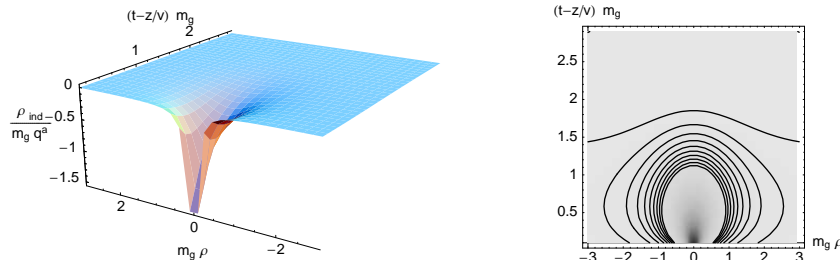


Fig. 3. Spatial distribution of the induced charge density for a color charge traveling with velocity $v/c = 0.99$ in a high temperature QCD plasma where the HTL approximation applies. The left plot shows equi-charge density lines in the rest frame of the charge.

Again, the components of the current density are proportional to m_g^3 .

For the dispersion relations (18), longitudinal and transverse plasma modes can only appear in the time-like sector of the ω, k plane [19, 21]. Therefore, collective excitations do not contribute to the charge and current density profile of the wake. Emission analogous to Cherenkov radiation and Mach cones are absent, but the charge carries a screening color cloud along with it. Fig. 3, which shows the charge density of a colored parton traveling with $v = 0.99c$, illustrates this physically intuitive result.

In spite of the absence of a Mach cone, the particle loses energy due to elastic collisions in the medium, which can be described by formula (15). This mechanism of energy dissipation has been studied in [23]. The integrand in (15) contributes to the integral in the space-like region only, where $|x| < 1$, and hence does not get contributions from frequencies where collective plasma modes exist. This is consistent with the fact that such modes are not excited by the moving color charge.

5. Charge wake induced in a strongly coupled QGP

In the second scenario we investigate what happens if the QCD plasma is a strongly coupled quark-gluon plasma (sQGP) that can be described as a quantum liquid. Our consideration of the second scenario is motivated by the RHIC experimental results on collective flow, which have led to the conclusion that the QCD plasma behaves like a nearly ideal fluid with very low viscosity (see e. g. [36]). This implies that long wavelength collective modes are almost undamped, while the short-distance dynamics are strongly dissipative due to large transport cross sections. In this respect, the sQGP resembles the electron plasma in metallic targets described in the previous section. The idea that a fast parton could excite Mach waves in such a QCD plasma and that the sound velocity of the expanding plasma could be determined from the emission pattern of the secondary particles traveling at an angle with respect to the jet axis was first suggested by Stöcker [37]. The recent work by Casalderrey-Solana and Shuryak [38] explores the formation of a conical flow by a hard parton in a quark-gluon plasma within a hydrodynamical framework, but does not specify

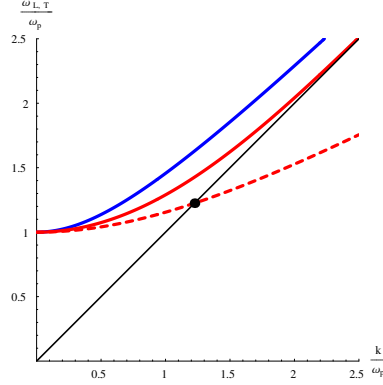


Fig. 4. Dispersion relation for the plasmon mode for a weakly coupled plasma described by the HTL formalism (solid red line) and for a strongly coupled plasma described by the modified Bloch formula (24). The latter extends into the space-like region ($k > \omega$) of the $\omega - k$ plane. The dispersion curve of transverse HTL-plasma modes is shown in blue and the light cone ($\omega = k$) is represented in black. The black dot indicates the point k_s where the dispersion curve intersects the light cone.

how the energy of the quenched jet is deposited into the medium.

There are presently no theoretical methods available for first principle calculations of the color response functions in a strong coupled QGP plasma. We therefore confine our investigation to a simple model, which encodes the essential differences between a quantum liquid scenario and the weak coupling scenario of the last section. The most prominent difference is the possibility that a plasmon mode may extend into the space-like region of the $\omega - k$ plane above some threshold value k_s . As we already emphasized, the sQGP paradigm suggests very low dissipation at small k , but large dissipation at high k . Our assumption is that a critical momentum k_c separates the regimes of collective and single particle excitation modes in the quantum liquid where the dominant colored modes below k_c are plasmon excitations with negligible dissipative single-particle coupling. Since we are here predominantly interested in collective effects in the plasma, we restrict our study to the region $k < k_c$ and simply cut off all Fourier integrals at k_c .

To be specific, we assume that the dielectric function of the strongly coupled plasma in the $k < k_c$ regime leads to a longitudinal dispersion relation of the form:

$$\omega_L = \sqrt{u^2 k^2 + \omega_p^2}, \quad (23)$$

where ω_p denotes the plasma frequency and $u < c$ is the speed of plasmon propagation, here assumed to be constant. In accordance with (23) we posit the following dielectric function

$$\epsilon_L = 1 + \frac{\omega_p^2/2}{u^2 k^2 - \omega^2 + \omega_p^2/2} \quad (k \leq k_c), \quad (24)$$

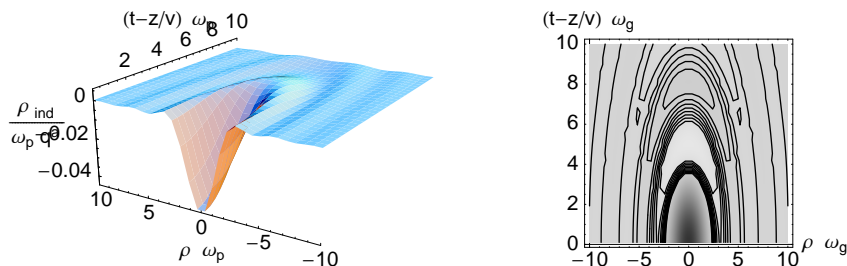


Fig. 5. Spatial distribution of a induced charge density around a color charge traveling with velocity $v = 0.55c < u$. The left plot shows equi-charge density lines. The density profile is similar to that of the cloud surrounding a color charge at rest.

which differs from the classical, hydrodynamical dielectric function of Bloch [28] by remaining regular in the limit $k, \omega \rightarrow 0$. The Bloch function is singular at small k, ω due to the mixing of the plasmon mode with the phonon mode. Such a mixing cannot occur in the QCD plasma, because the plasmon and phonon belong to different irreducible representations (octet versus singlet) of color SU(3) and because the medium is charge symmetric.

The dielectric function (24) is constructed in such a way that it allows us to study one specific aspect of a quantum liquid scenario: that the plasmon mode may extend into the space-like region of the $\omega - k$ plane. This behavior is illustrated in Fig. 4 by the dashed red line, which cuts through the light cone at k_s (at the black dot in Fig. 4) and continues into the space-like region. This contrasts with the dispersion relation of the longitudinal plasmon mode in the HTL formalism (solid red line), which always remains in the time-like region $\omega(k) > k$. The induced wake structure for a supersonically (in the sense $v > u$) traveling color source in such a quantum liquid scenario is, quite generally, a conical Mach wave structure. The principal findings of our study can be expected to hold for any quantum liquid with a plasmon branch similar to (23), independent of the exact form of the dielectric function. We here assume a speed of plasmon propagation $u/c = 1/\sqrt{3}$. This differs from the speed of plasmon propagation in the small k limit of the HTL approximation, $u/c = \sqrt{3}/5$ [21], and is also different from the sound velocity in a hadronic resonance gas $u/c \approx \sqrt{0.2}$ [39, 40].

Determining the plasmon mode via Eq. (23) reveals that the mode is in the space-like region of the $\omega - k$ plane for $k > k_s = \omega_p/\sqrt{c^2 - u^2}$. Recall that this is different from the high-temperature plasma, where longitudinal and transverse plasma modes only appear in the time-like region, $|x| = |\omega/k| > 1$. In the quantum liquid scenario one can expect that the modes with low phase velocity $|x| < u/c$ suffer severe Landau damping because they accelerate the slower moving charges and decelerate those moving faster than the wave. A charge moving with a velocity lower than the speed of plasmon propagation can only excite those modes and not the modes with intermediate phase velocities $u/c < |x| < 1$, which are undamped [18, 21]. In this case, the qualitative properties of the color wake are analogous to those of the high temperature plasma: the charge carries a localized screening color cloud

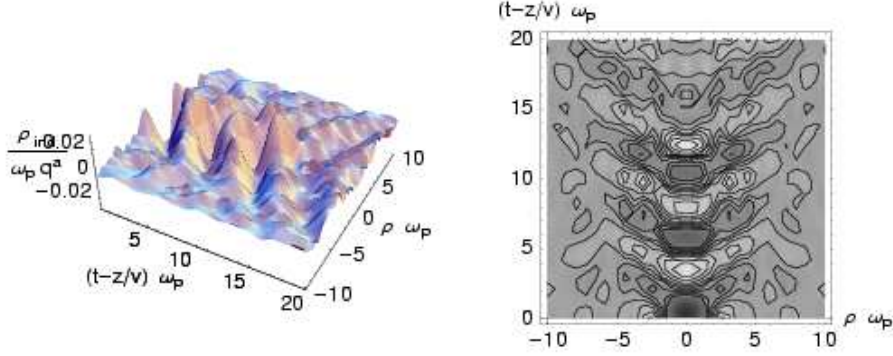


Fig. 6. (a) Spatial distribution of the induced charge density from a jet with high momentum and fixed color charge q^a that is traveling with $v = 0.99c > u = \sqrt{1/3}c$. (b) Plot showing equi-charge lines in the density distribution for the situation in (a).

with it and Cherenkov emission and Mach cones are absent. Using (20) and restricting the integration area to the region $k < k_c = 2\omega_p$, one can illustrate this for a colored parton traveling with $v = 0.55c < u$. Figure 5 shows the charge density cloud traveling with the colored parton.

If the colored parton travels with a velocity v that is higher than the speed of plasmon propagation u , modes with an intermediate phase velocity $u/c < |x| < 1$ can be excited. The emission of these plasma oscillations induced by supersonically traveling particles is analogous to Cherenkov radiation, but different in that the density waves are longitudinal, not transverse, excitations of the color field. Figure 6 for a color charge traveling with $v/c = 0.99$ clearly exhibits the emergence of Mach cones in the induced charge density with an opening angle given by the Mach relation (17).

We emphasize that the existence of Mach cones is expected in a plasma in general if the particle is moving faster than the speed of sound in the plasma and if the dispersion relation of the collective mode extends into the space-like region. The wake induced by a colored jet in such a setting leads to regions of enhanced and depleted charge density in the wake, which have the shape of Mach waves trailing the projectile.

6. Summary and Outlook

We have calculated the properties of the color charge density wake of a hard parton traveling through a quark-gluon plasma in linear response theory for two different scenarios: a weakly coupled QGP at $T \gg T_c$ described in the HTL approximation, and a strongly coupled QGP with the properties of a quantum liquid. We found that the wake in the weakly coupled plasma always takes the form of a screening cloud traveling with the particle, while the wake in the strongly coupled plasma assumes the form of a Mach cone, if the parton's velocity exceeds the speed of plasmon propagation and the collective plasma mode has a

dispersion relation extending into the space-like region.

In general, secondary particle distributions can be used to probe the collective excitations QCD plasma. If these take the form of Mach cones they should reveal themselves by the directed emission of secondary particles from the plasma, similar to what was observed with metallic targets under bombardment by swift ions. If the scenario of a strongly coupled QCD plasma is realized in relativistic heavy ion collisions, one can expect to observe these cones in the angular distribution of secondary particles associated with jets [37, 38]. As we already mentioned in the introduction, preliminary data from the RHIC experiments (see e. g. Fig. 1 in [13, 14]) suggest that the angular distribution of secondary hadrons in the direction opposite to an energetic hadron is peaked at an azimuthal angle $\Delta\phi \neq \pi$. This is different from what is observed in $p + p$ collisions, where the maximum associated with the away-side jet is clearly located at $\Delta\phi = \pi$. In contrast, two maxima are located at $\Delta\phi \approx \pi \pm 1.1$ in Au + Au collisions. This phenomenon suggests the presence of a Mach shock front traveling with the quenched away-side jet at an angle $\Delta\phi = \pi \pm \phi_M = \pi \pm \arccos(u/v)$.

If these speculations are confirmed, it will be an interesting theoretical problem to determine the mechanism that excites the shock front. Possible candidates are the collective plasma excitations discussed here [16, 37], the “thunder” effect following localized directed energy deposition by the quenched jet [38], or simply the knock-on process due to elastic collisions of plasma particles with the away-side hard parton [41].

Acknowledgements

This work was supported in part by U. S. Department of Energy under grant DE-FG02-05ER41367. JR thanks the Alexander von Humboldt Foundation for support as a Feodor Lynen Fellow. BM gratefully acknowledges partial support from GSI to attend this Symposium.

References

1. J. D. Bjorken, FERMILAB-PUB-82-059-THY (unpublished).
2. M. Gyulassy and M. Plümer, Phys. Lett. B **243**, 432 (1990).
3. X. N. Wang and M. Gyulassy, Phys. Rev. Lett. **68**, 1480 (1992).
4. K. Adcox *et al.* [PHENIX Collaboration], Phys. Rev. Lett. **88**, 022301 (2002)
5. C. Adler *et al.* [STAR Collaboration], Phys. Rev. Lett. **90**, 082302 (2003)
6. J. Adams *et al.* [STAR Collaboration], Phys. Rev. Lett. **91**, 172302 (2003)
7. R. Baier, D. Schiff and B. G. Zakharov, Ann. Rev. Nucl. Part. Sci. **50**, 37 (2000)
8. A. Kovner and U. A. Wiedemann, arXiv:hep-ph/0304151.
9. A. Accardi *et al.*, arXiv:hep-ph/0310274.
10. P. Jacobs and X. N. Wang, Prog. Part. Nucl. Phys. **54**, 443 (2005)
11. J. Adams *et al.* [STAR Collaboration], arXiv:nucl-ex/0408012.
12. F. Wang [STAR Collaboration], J. Phys. G **30**, S1299 (2004)

13. J. Rak [PHENIX Collaboration], J. Phys. G **31**, S541 (2005).
14. S. S. Adler [PHENIX Collaboration], arXiv:nucl-ex/0507004.
15. J. Adams *et al.* [STAR Collaboration], arXiv:nucl-ex/0411003.
16. J. Ruppert and B. Muller, Phys. Lett. B **618**, 123 (2005) [arXiv:hep-ph/0503158].
17. J. Ruppert, arXiv:hep-ph/0506328.
18. S. Ichimaru, *Basic Principles of Plasma Physics*, (W. A. Benjamin, Inc., Advanced Book Program, 1973).
19. M. LeBellac, *Thermal Field Theory*, (Cambridge University Press, Cambridge, 2000).
20. J. Neufeld and R. H. Ritchie, Phys. Rev. **98**, 1632 (1955).
21. H. A. Weldon, Phys. Rev. D **26**, 1394 (1982).
22. V. V. Klimov, Sov. Phys. JETP **55**, 199 (1982).
23. M. H. Thoma and M. Gyulassy, Nucl. Phys. B **351**, 491 (1991).
24. H. J. Frischkorn, K. O. Groeneveld, S. Schumann, R. Latz, G. Reichhardt, J. Schader, W. Kronast and R. Mann, Phys. Lett. A **76**, 155 (1980).
25. M. Burkhard, H. Rothard, C. Biedermann, J. Kemmler, K. Kroneberger, P. Koschar, O. Heil and K. O. Groeneveld, Phys. Rev. Lett. **58**, 1773 (1987).
26. W. Schäfer, H. Stöcker, B. Müller and W. Greiner, Z. Phys. A **288**, 349 (1990).
27. W. Schäfer, H. Stöcker, B. Müller and W. Greiner, Z. Phys. B **36**, 319 (1980).
28. F. Bloch, Z. Phys. **81**, 363 (1933).
29. A. E. Glassgold, W. Heckroth and K. M. Watson, Ann. Phys. (Paris) **6**, 1 (1959).
30. W. Scheid, H. Müller and W. Greiner, Phys. Rev. Lett. **32**, 741 (1974).
31. H. Rothard *et al.*, J. Physique **48-C9**, 211 (1987); M. F. Burkhard, H. Rothard and K. O. Groeneveld, Phys. Stat. sol. **B147**, 589 (1988); H. Rothard *et al.*, J. Physique **50-C2**, 105 (1989); K. O. Groeneveld, R. Maier and H. Rothard, Il Nuovo Cimento **D12**, 843 (1990); H. Rothard *et al.*, Nucl. Instr. Meth. B **48**, 616 (1990); H. Rothard *et al.*, Nucl. Instr. Meth. B **56/57**, 843 (1991); H. Rothard, M. Schosnig, K. Kroneberger and K. O. Groeneveld, Phys. Rev. B **46**, 11847 (1992).
32. H. Rothard, Scanning Microscopy **9**, 1 (1995); Nucl. Instr. Meth. B **225**, 27 (2004); Radiotherapy and Oncology **73**, Suppl. 2, S105 (2005).
33. D. Normile, Science **278**, 1884 (1997).
34. R. D. Pisarski, Physica A **158** (1989) 146.
35. E. Braaten and R. D. Pisarski, Nucl. Phys. B **337**, 569 (1990).
36. D. Teaney, Phys. Rev. C **68**, 034913 (2003).
37. H. Stöcker, Nucl. Phys. A **750**, 121 (2005) [arXiv:nucl-th/0406018].
38. J. Casalderrey-Solana, E. V. Shuryak and D. Teaney, arXiv:hep-ph/0411315.
39. E. V. Shuryak, Yad. Fiz. **16**, 395 (1972).
40. R. Venugopalan and M. Prakash, Nucl. Phys. A **546**, 718 (1992).
41. I. P. Lokhtin and A. M. Snigirev, Phys. Lett. B **440**, 163 (1998) [arXiv:hep-ph/9805292].